#### **NURETH14-283**

# VALIDATION AND APPLICATION OF 3D-METHODS FOR THE DESIGN AND SAFETY ANALYSIS OF HIGH TEMPERATURE REACTORS

J. Bader<sup>1,2</sup>, J. Lapins<sup>2</sup>, M. Buck<sup>2</sup>, W. Bernnat<sup>2</sup> and E. Laurien<sup>2</sup>

<sup>1</sup> EnBW Kernkraft GmbH, Kernkraftwerk Philippsburg, Rheinschanzinsel, Philippsburg, Germany

<sup>2</sup> Institute for Nuclear Technology and Energy Systems (IKE), University of Stuttgart, Germany

Corresponding author: johannes.bader@ike.uni-stuttgart.de

#### **Abstract**

Some of the concepts for future nuclear reactors are high-temperature gas-cooled reactors. Previous simulation codes for their cores were often based on one- or two-dimensional models, but today's increasing computer capabilities make an advance to 3D-codes possible now. Our thermal-hydraulic code ATTICA3D (Advanced Thermal-hydraulic Tool for In-vessel and Core Analysis in 3 Dimensions) is based on the porous media approach, including 3-D models of heat conduction and gas flow, using a coarse-grid integration method for the time-dependent conservation equations of mass, momentum and energy.

Results of numerical calculations for various validation cases are presented: First, the test facility SANA is chosen, which has been used to study heat transfer phenomena inside a coolant-gas filled pebble-bed core, which was heated by embedded electrical heating elements. Calculations were carried out for different tests taken from the experimental database. Measured and calculated temperatures at different positions are compared and found in good agreement.

Second, our code was used to simulate a depressurized loss of forced cooling experiment with simulated decay heat in the AVR Experimental Reactor. Due to its design with the shut-down rods located inside columnar noses, which extend into the pebble bed of the core, geometry and power distribution are genuinely three-dimensional. The power distribution was calculated by the 3D-Neutronic Diffusion Code CITATION in conjunction with the spectral code MICROX-2. The neutronics and thermal-hydraulics calculations were carried out for a 3D, 45°-degree section of the reactor. It is demonstrated, that the experimental results could be qualitatively reproduced.

**Keywords:** Thermal-hydraulics, code validation, neutronics, high temperature gas cooled reactor, AVR

#### 1. Introduction

For the future of nuclear energy, the GEN-IV Forum [1] defined six promising future reactor concepts. Two of these are gas cooled reactors, one is the Gas Cooled Fast Reactor (using a fast neutron spectrum), and the other one is the Very High Temperature Reactor (graphite-moderated for a thermal spectrum). Therefore, tools have to be provided to analyse and design these future concepts.

Gas cooled high temperature reactor concepts have been developed for some time now. In most of the previous works two-dimensional codes were involved in the design analysis with geometrical simplified models [2]. Recently, also detailed but time consuming simulations using three-dimensional CFD-Methods [3] were introduced. Three-dimensional codes are necessary for the analysis of various problems related to design optimization and safety analysis in gas-cooled nuclear reactors, e.g. the non-axisymmetric withdrawal of control rods or a fuel inventory with non-uniformly distributed burn-up. Increasing computational capabilities make three-dimensional approaches more and more feasibly, especially when they are combined with adequately averaged models for the heat transfer and the gas behaviour, which allow the use of relatively coarse meshes.

The three-dimensional thermal-hydraulics code ATTICA3D, which we had previously introduced as TH3D [4] [5], is based on the porous media approach for the description of the fluid flow and the heat transport in high-temperature gas-cooled reactors. Up to now, mostly results of code to code comparison have been published. The present paper concentrates on the validation of the code by comparisons with experimental results.

### 2. Mathematical-Physical Model

In ATTICA3D, the gas and solid phase inside a volume mesh are treated as continua, described by the porosity of the cell. Multiple gas types are implemented and can be used. Their properties are calculated as a function of pressure and temperature. ATTICA3D simulation grid can use cylindrical or cartesian coordinates. The time dependent, compressible mass conservation equation is solved for the gas phase:

$$\varepsilon \frac{\partial}{\partial t} \rho_g + div \left( \varepsilon \rho_g \vec{u} \right) = 0 \tag{1}$$

In (equation 1),  $\varepsilon$  denotes the isotropic porosity,  $\rho_g$  the density of the gas, and  $\vec{u}$  the velocity vector. The mass diffusion is presently not considered. The momentum equation is expressed by a simplified, steady-state approach according to Ergun [6]:

$$\varepsilon \, \overrightarrow{grad}(p) = -\vec{R} - \varepsilon \rho_g \, \vec{g} \tag{2}$$

Here, p denotes the pressure,  $\vec{R}$  the friction forces (after Colebrook) and  $\vec{g}$  the gravitational acceleration. The simplified equation can be formulated due to the fact that friction forces and gravity body force are dominating over the inertial force. Two energy equations assuming thermal non-equilibrium between solid and gas phase are solved (equation 3 and equation 4):

$$(1 - \varepsilon) \frac{\partial}{\partial t} (\rho_s h_s) = div((1 - \varepsilon)\lambda_s \overrightarrow{grad}(T_s)) - \dot{q}_{conv} + \dot{q}_{nuclear}$$
(3)

$$\varepsilon \frac{\partial}{\partial t} (\rho_g h_g) + div(\varepsilon \rho_g \vec{u} h_g) = div(\varepsilon \lambda_g \overrightarrow{grad}(T_g)) + \dot{q}_{conv}$$
(4)

Here, hs and hg denote the enthalpy of the solid and gas, Ts and Tg the solid and gas temperature,  $\lambda$ s and  $\lambda$ g the effective heat conductivities of solid and gas, and  $\dot{q}_{conv}$  and  $\dot{q}_{nuclear}$  volumetric heat sources due to convective heat exchange and nuclear heating, respectively. The heat transfer by radiation is considered in gaps by the Stefan-Boltzmann law, heat transfer for laminar and turbulent flow in every mesh (not in the pebble bed) is considered by specific correlations of the Nusselt number. The pressure drop in the pebble bed is calculated by the KTA-Rule [7]. Here, the porosity, the diameter

of the pebbles, the mass flow and the density of the fluid are taken into account with an correlation of the friction factor.

Several fluids like helium, air, nitrogen are implemented with their properties. Thermal dispersion inside the pebble bed is considered after a correlation from Bauer [9] The friction forces of the flow are calculated according to a smooth pipe approach after hydraulic parameters given in the input. A Zehner-Schlünder-Robold [8] model is used for calculating the heat transfer in the pebble bed, which includes a fraction of heat transfer by radiation, by convection and conduction .

The system of conservation equations is transformed into an initial value problem for a set of ordinary differential equations by applying the Finite Volume method for a structured grid to discretize the spatial derivatives. A staggered grid approach is applied, where scalar variables (pressure, enthalpies) are located at the centre of control volumes. The velocity of the fluid is calculated at cell faces. For time integration, a fully implicit, time adaptive multi-step backward differentiation method (BDF) is used. The non-linear equations produced by BDF are subsequently solved for each time step by a modified Newton-Raphson method together with sparse matrix techniques.

A heterogonous fuel model is implemented to determine the neutron feedback of the temperature. Since the feedback for HTRs is divided into fuel, moderator and reflector coefficient, it is necessary to know the related temperatures. For that purpose, the average fuel and moderator temperature are calculated by a spherical model of arbitrary shells using the solid temperature of the cell as the outer boundary condition. The neutronic code uses the achieved temperatures for the calculation of the power, which is then assigned back to the thermal-hydraulic code. Some promising results of the coupling have already been shown in [10].

#### 3. Validation calculations

## 3.1. Calculations for SANA experiments

# 3.1.1. Description of the SANA facility

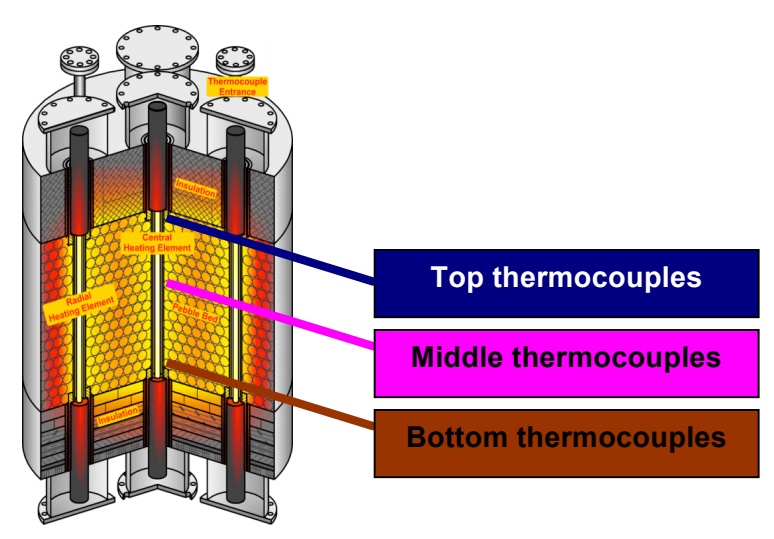


Figure 1: SANA test facility

The SANA test facility, acronym for "Selbsttätige Abfuhr der Nachwärme" (test facility for demonstration of safe decay heat removal by passive means), was built at the Forschungszentrum Jülich (FZJ) [11][12] to provide an experimental data base for the validation of thermal-hydraulic codes for pebble beds (Figure 1). Several pebble sizes and pebble materials were tested with different gases and different eclectrical heating powers in steps to 5, 10, 20, 25, 30 and 35 kW (Table 1). Since

the goal was to investigate the heat transfer under depressurised accident conditions, no forced flow trough the pebble bed was applied (except low mass flow for compensating leakage losses) under a pressure of ambient conditions. In order to avoid heat losses in axial direction, the top and bottom of the steel containment were insulated by fiber materials. All these experiments were performed with a central rod-like electrical heating element. Three additional heating elements, each with a power up to 5 kW, could be inserted into the pebble bed (Table 1). Thermocouples were installed on the surface of the vessel, the insulation layers and the pebble bed to obtain the desired data.

Maximum pebble bed temperature	1600 °C	Complete height	3.2 m
Installed electrical power	35 kW + 3 x 5 kW	Gas inside pebble bed	Helium, Nitrogen
Diameter of pebble bed	1.5 m	Pebble diameter	60mm, 30mm
Height of pebble bed	1.0 m	Pebble material	Graphite, Aluminum

Table 1: Basic data of the SANA test facility

#### 3.1.2. Calculations for selected SANA tests

Two different representations of the SANA facility are applied in our analyses: a simplified and a detailed model. The simplified model is used to achieve short computational time, whereas the detailed model was used to gather more detailed information. Both models consist of a 15° section of the cylindrical facility. The porosity of the pebble bed is modelled according to the data provided for the experiment. For the material properties of the pebble bed and the insulation layers data (heat conductivity, emissivity etc.) given in the reports describing the experiments were applied.

The simplified model consists of the pebble bed as well as the top and bottom insulation layers using a total of 320 cells.

Although the SANA tests were carried at atmospheric pressure, where effects of convective heat transport are at a minimum, the steady state temperature distributions obtained in the experiments show effects, which can only be explained by a natural convection flow inside the pebble bed. In order to demonstrate this, a series of calculations is presented for an experiment with a centrally heated pebble bed, composed of 60 mm graphite balls in a Helium atmosphere with a nominal heating power of 10 kW. The heat conductivity of the 60 mm graphite pebbles differs from 152.3 W/mK at 100°C to 55 W/mK at 1000°C. The emissivity is supposed to be constant with a value of 0.9.

Three different types of calculations were performed: The first calculation was performed without any gas inside the pebble bed, which means that the solution of this problem is only a heat conduction problem. The second calculation was done with calculation of natural convection flow inside a pebble bed with uniform porosity (0.39). In a third calculation the effects of the channelling near the bordering walls was additionally taken into account, as suggested in [12]. Since the porosity of the pebble bed is bigger near the bounding walls, the flow resistance in this area is smaller. Hence, the channelling has an influence on the heat transfer in the pebble bed. Figure 2 shows a comparison between the flow of the pebble bed without and with channelling in a helium atmosphere. The higher velocity of the gas close to the heating element and the vessel wall is obvious. Figure 3 shows the comparison with measured temperatures for the different calculations.

The heat transfer inside the pebble bed is significantly influenced by the convective heat transfer of the fluid, even at atmospheric pressure. This can be seen in the result of the first calculation, where only conduction and radiation were considered. While the radial temperature profile is approximately reproduced, the axial temperature differences obtained in the experiment are not. This is only possible by calculating the natural convection flow in addition. A further improvement regarding the

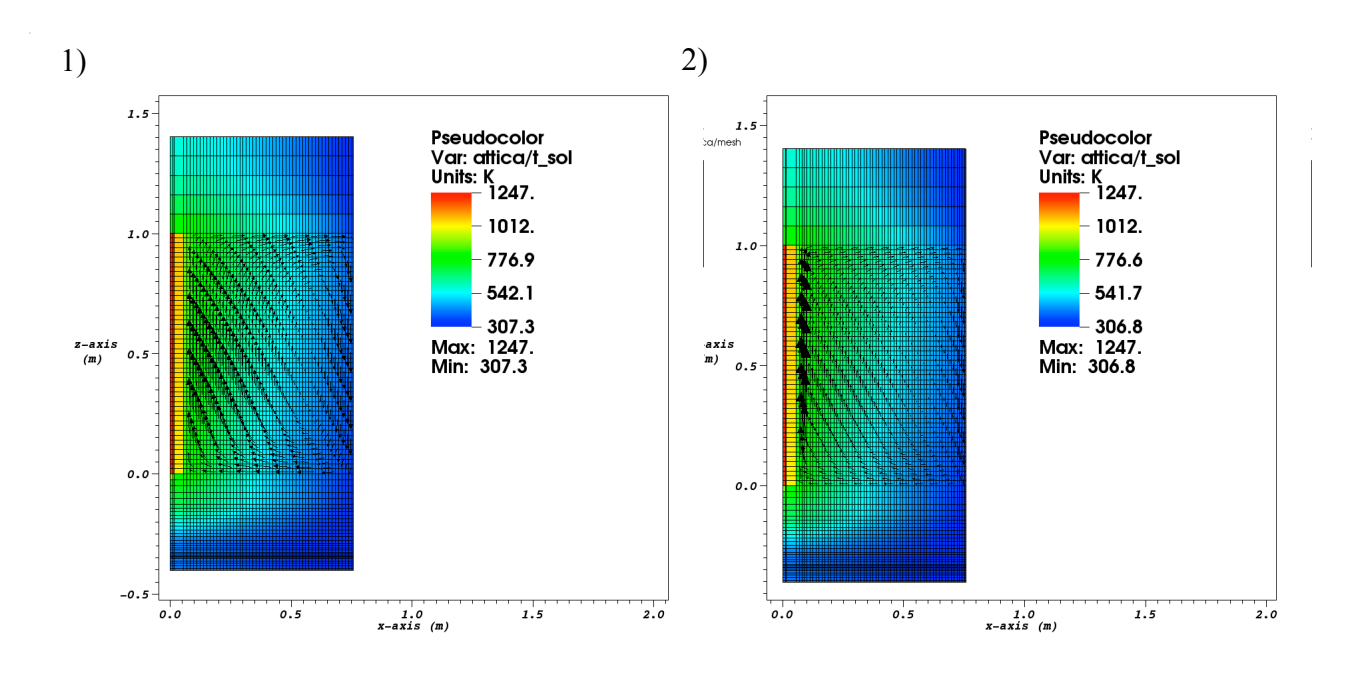


Figure 2: Temperature distribution of solid temperature for simple SANA simulation model with convective flow: 1) without channelling, 2) with channelling

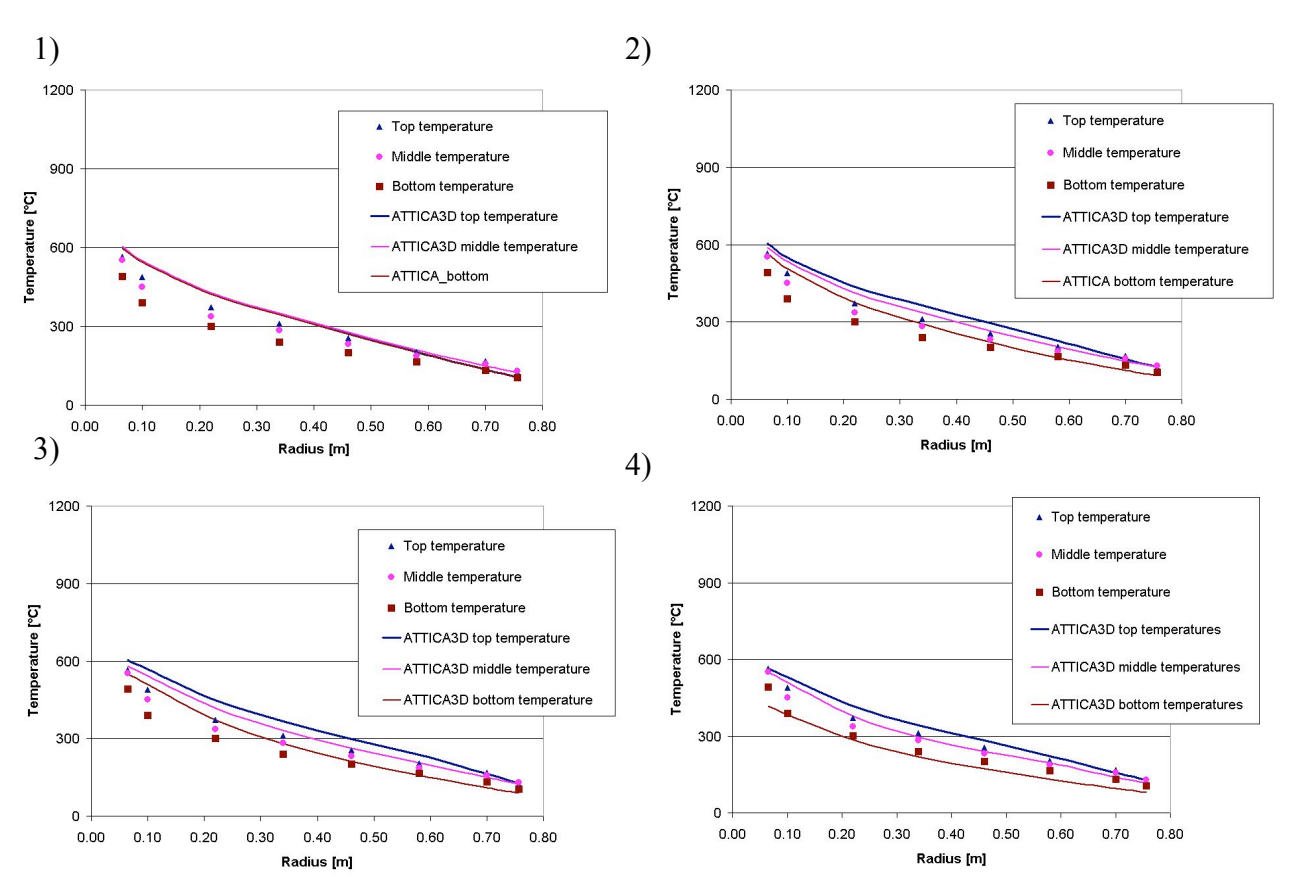


Figure 3: Comparison of SANA temperatures for 10 kW: 1) only heat transfer, 2) without channelling, 3) with channelling, 4) detailed model

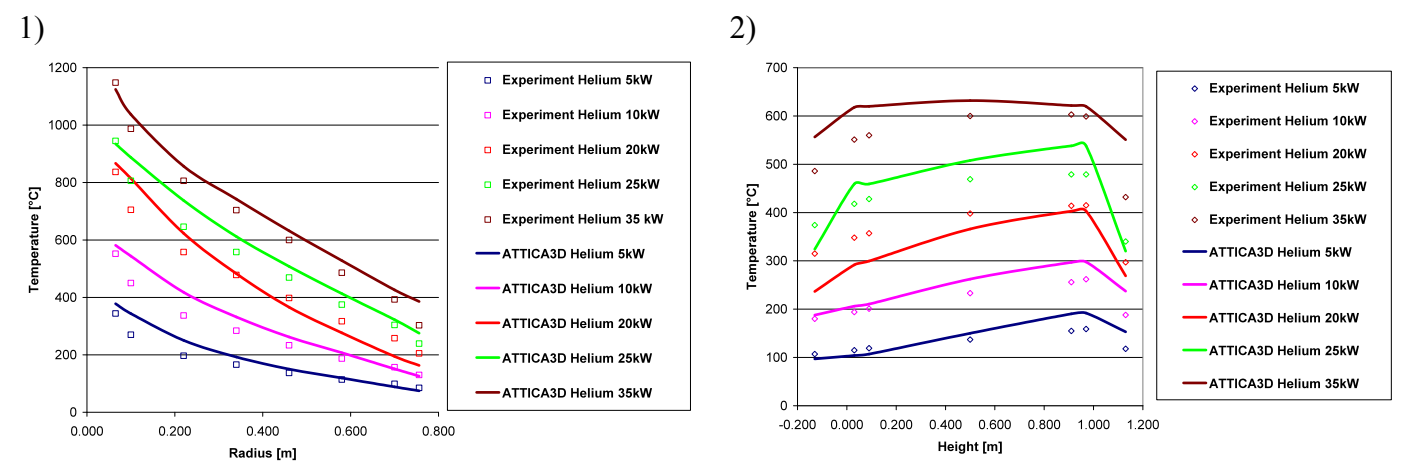


Figure 4: Comparison of results for SANA for Helium: 1) vertical profiles for radius of 46cm, 2) horizontal profiles at height of 50cm

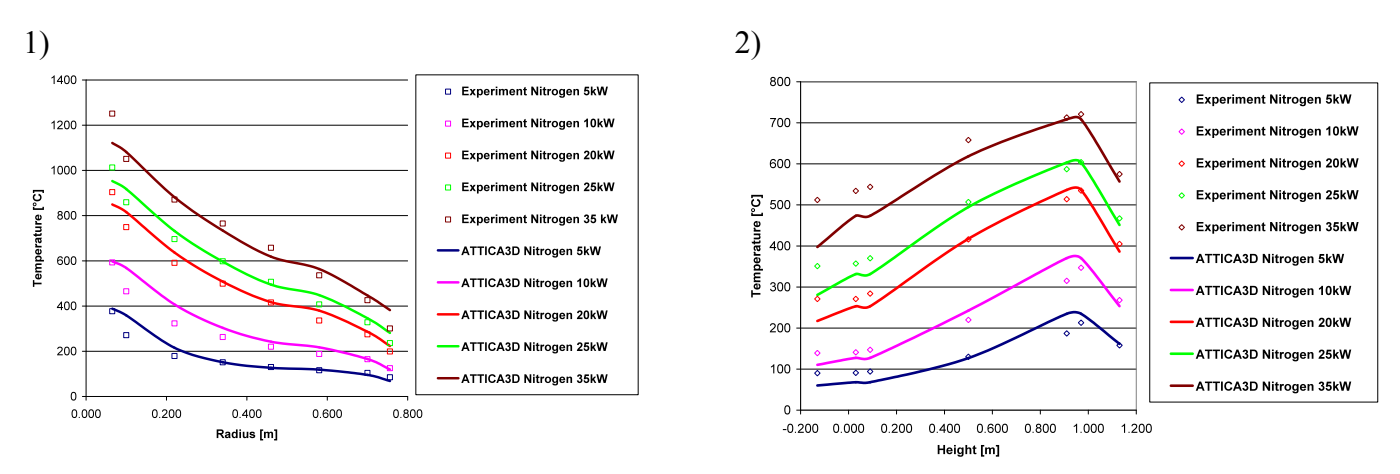


Figure 5: Comparison of results for SANA for Nitrogen: 1) vertical profiles for radius of 46cm, 2) axial profiles at height of 50 cm

comparison with the experiment is seen if the channelling effect is considered, which enhances the impact of convective heat transport. Even better agreement with experimental results can be achieved with a more detailed representation of the experimental geometry, as can be seen from the result for a refined mesh with 980 cells also included in Figure 3, which additionally accounts for the water-cooled heating electrode as a boundary condition.

A summary of our calculations with different heating powers in beds composed of 60 mm graphite pebbles is given in Figure 4 for tests in Helium atmosphere and in Figure 5 for tests in Nitrogen atmosphere. Due to the lower heat conductivity of Nitrogen, the effect of convection is more important as compared to Helium, what can be seen in the measured axial temperature profile. This trend is correctly reproduced be the ATTICA3D calculations. In general, the comparison of the calculations with the experimental results shows good agreement and is improving with increasingly detailed descriptions. Further calculations are planned with improved representation of experimental boundary conditions, although these are partly difficult to determine from the available reports.

## 3.2. AVR Experimental High Temperature Reactor

3.2.1. Description of the AVR

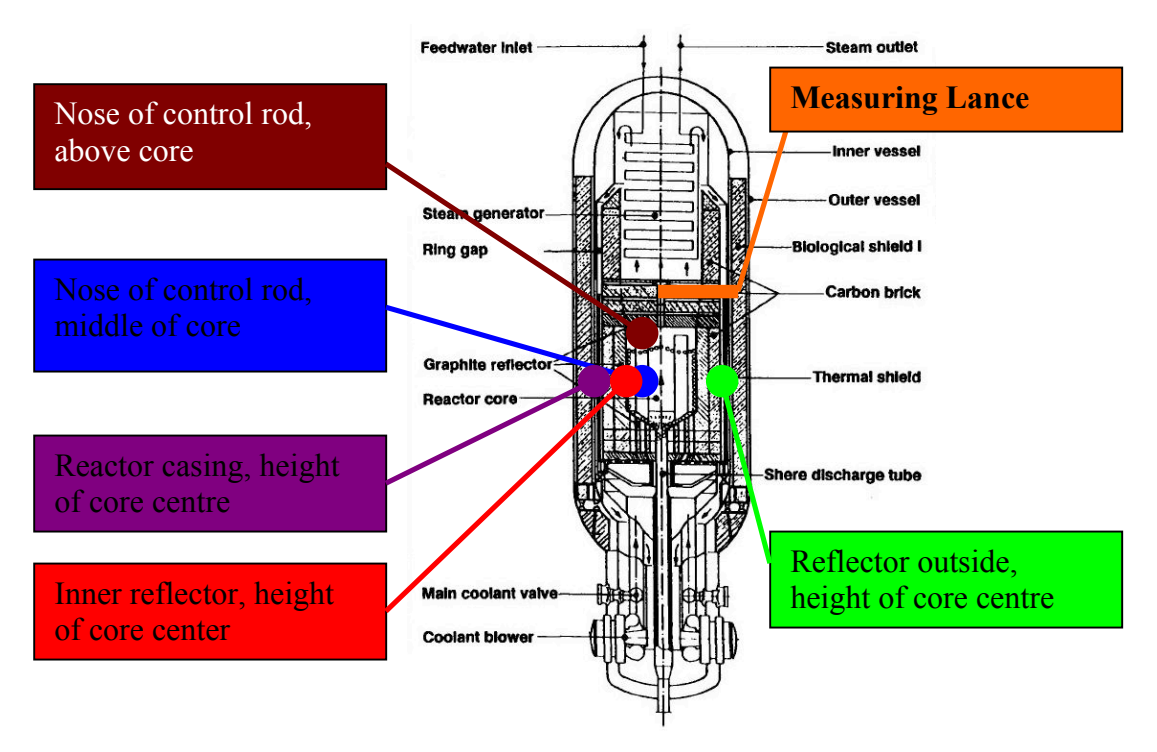


Figure 6: AVR experimental reactor with locations of temperature measurement.

Core diameter	3.0 m	Mass flow	13 kg s <sup>-1</sup>
Average core height	2.8 m	Loop pressure	10.8 bar
Thermal power	46 MW	Diameter of fuel elements	6 cm
Average power density	2.6 MW/m <sup>3</sup>	Inlet temperature	270 °C
		Outlet temperature	950 °C

Table 2: AVR basic data

The AVR experimental high-temperature reactor was constructed and operated at the FZJ as a pebble-bed-type research reactor [13] [14]. The coolant Helium circulated with a pressure of 10.8 bars within a primary loop driven by two circulators. One of the characteristics that distinguished the AVR from newer designs was that the coolant flowed from the bottom to the top through the pebble bed. A steam generator was situated inside the same pressure vessel as the pebble bed to achieve a compact design of the whole setup (Figure 6). The pebble bed consisted of approximately 100,000 pebbles with a diameter of 6 cm. Different types of fuel elements for test purposes were used [15]. The basic design parameters are shown in Table 2. One of the specialties of the AVR was the positioning of control rods: they were inserted within graphite noses which extend into the pebble bed. The AVR was operated for 21 years and many safety related experiments were performed.

#### 3.2.2. Experiment for depressurized loss of coolant accident

One of the performed experiments was the simulation of a depressurized loss of coolant accident (DLOFCA) [16] with passive removal of decay heat. Under normal operational conditions, the pebbles were brought continuously onto the top of the core by a pneumatic feeding system. For this test, the feed of new pebbles was stopped until the reactor power dropped to 4 MW. The pressure of the coolant loop was reduced from 10.8 bars to 1 bar to achieve temperatures similar to nominal operation. Further

initial conditions of the experiment are shown in Table 3. For the experiment, the helium circulators were shut down and the reactor power was then regulated by the control rods to achieve a power development equivalent to the decay heat. The test was performed once with open and once with closed circulator valves. This was done to assure that the main heat transport mechanism is directed radially in the pressure vessel, as opposed through a natural vertical convection loop of gas. However, since the steam generator was still cooled with water for safety reasons, another major heat sink of the helium convection was still the steam generator.

Several thermocouples were installed during the construction of the AVR. It must be noted that the measured temperatures are not the same for different azimutal positions in spite of 90° symmetric structures. This behaviour could not be fully explained by the available data. For example, the measured temperature at the point "nose of control rod, middle" differs from 543 to 465 and 608 °C. This may imply an unsymmetrical flow as a starting condition due to the slots in the top reflector.

Thermal power	4 MW	Steam generator water mass flow	20 t/h
Average power density	2.6 MW/m <sup>3</sup>	Steam generator inlet temperature water	130 dropped to 60 °C
Inlet temperature	183 °C	Steam generator outlet temperature	256 dropped to 67 °C
Outlet temperature	810 °C	Mass flow	1.5 kg s <sup>-1</sup>

Table 3: Initial conditions of the AVR DLOFCA experiment

## 3.2.3. ATTICA3D calculation for the AVR DLOFCA experiment

The computational domain considered for the calculation was a 45° section of the AVR geometry, with a symmetry plane in the middle of the graphite nose at 45° (Figure 7). The ATTICA3D grid includes the side reflector with the Helium down-comers, the cold plenum below the core, the core itself with the graphite nose, the top reflector and a steam generator structure. The whole mesh consists of 17,298 volumes.

The power distribution of the AVR experiment was calculated by the three-dimensional multigroup diffusion code CITATION [18] in the framework of the RAPHAEL project [17]. Since nine different fuel element types were used in the AVR for experimental purposes, several calculation steps had to be made. The core was described by a data file consisting of 139 core zones, containing fractions of moderator balls, fuel elements of the nine types and 50 burn-up classes. For each core zone a mixture of pebbles with different structure, fuel and burn-up is considered. The spectral code MICROX-2 [19] was used to generate homogeneous macroscopic cross section data for the core zones. Since MICROX-2 can only process one type of fuel assembly, first separate spectral calculations for all core zones were performed for all types of assemblies contained in this zone. ATTICA3D provided the fuel and moderator temperatures of these zones. Then, the macroscopic cross sections for the different core zones were composed according to their fraction of element types. Additionally, the average burnup of each zone was used as basis for the spectral calculations. The final cross sections with a 26energy-group structure provided a detailed space and energy resolution of the neutron flux density distribution of the three-dimensional core. Temperature-dependent cross-section data for transient calculation were also prepared by MICROX-2. An iterative procedure with three times repeated calculations of the neutronic code CITATION and the thermal-hydraulic code ATTICA3D was applied to obtain a consistent steady state of power and temperature. It is assumed that the shape of the power distribution remains the same during the experimental transient. The 3D-shape is presented in Figure 8 with iso-

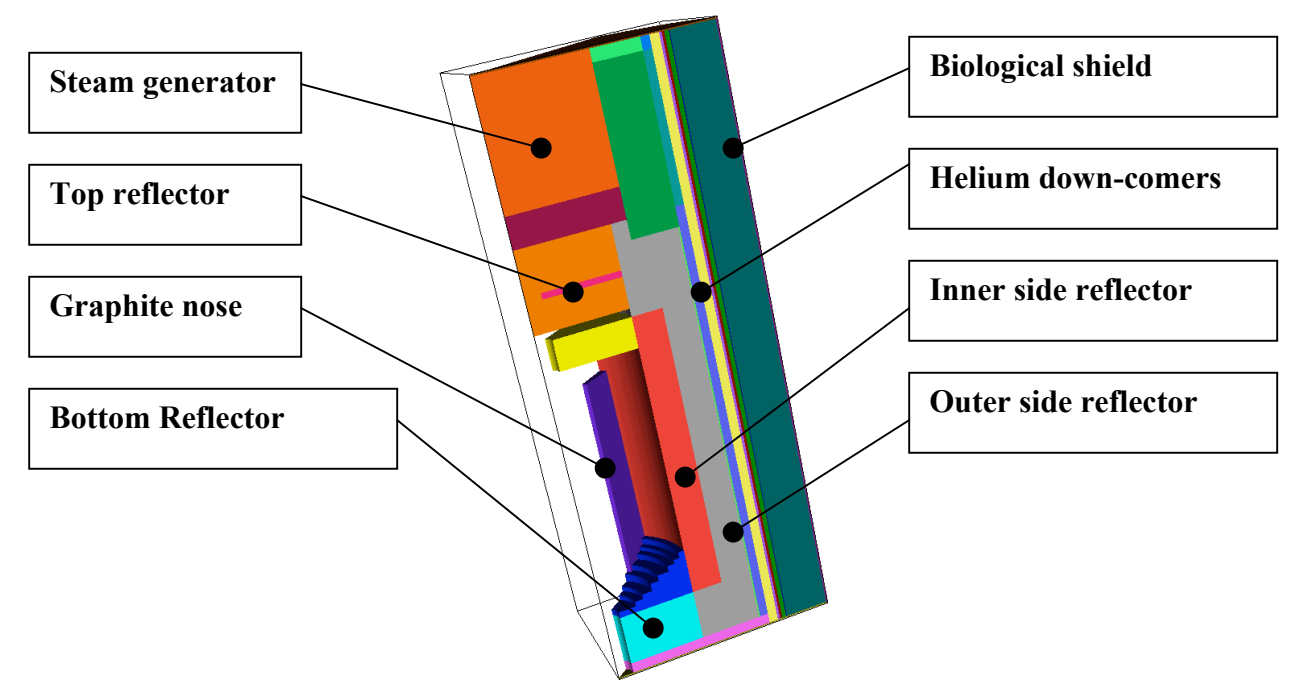


Figure 7: 3D model used for the ATTICA3D calculation for the AVR: 45° section with major geometrical structures

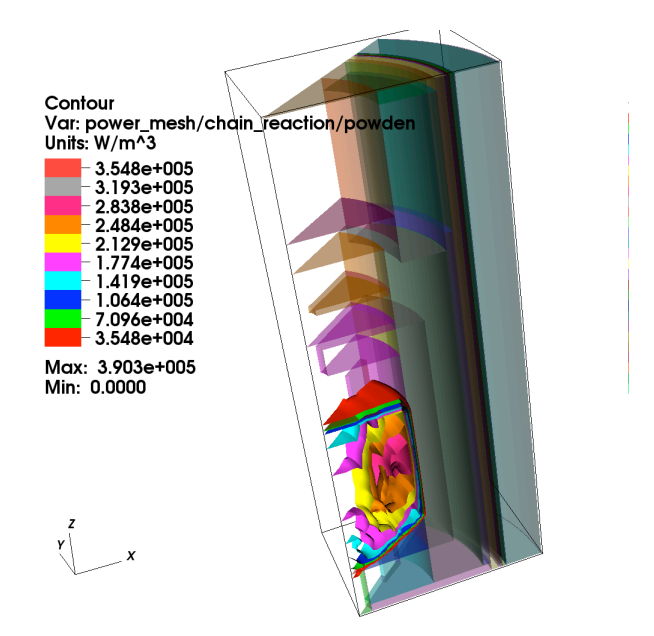


Figure 8: AVR power distribution within 3D-Geometry

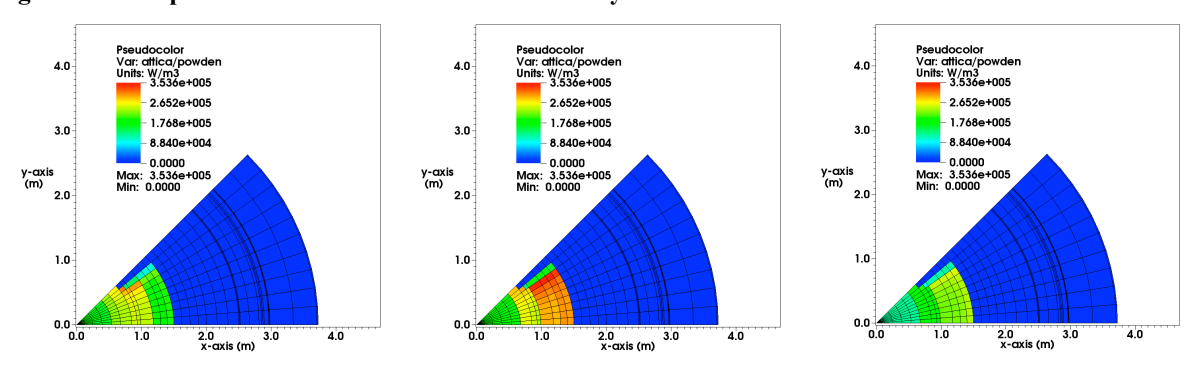


Figure 9: Cut of AVR power distribution at 0h in 1 m, 2 m and 3 m height of core

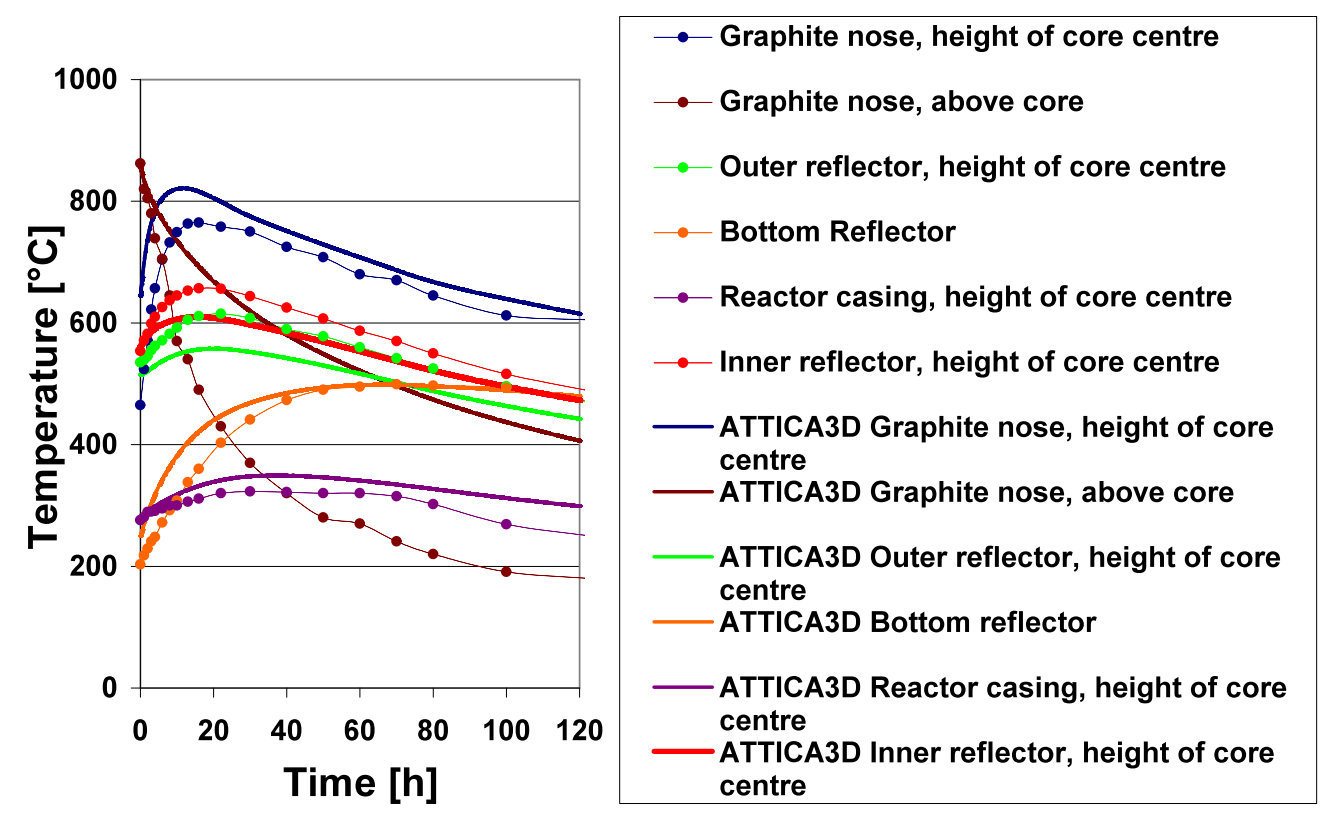


Figure 10: Development of measured and calculated temperatures during the AVR DLOFCA experiment

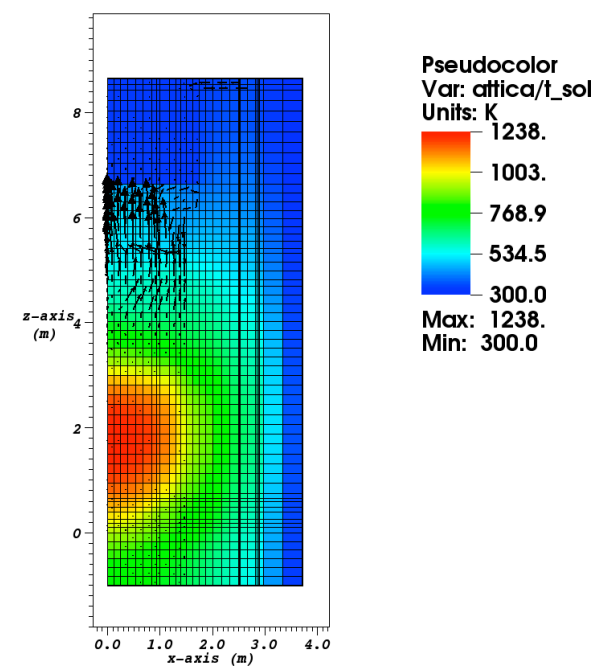


Figure 11: Solid temperature distribution (colour scale) and flow field (arrows) in the AVR experiment at 120h

surfaces, some plane sections through the distribution at 1 m, 2 m and 3 m above the upper edge of the cone of the pebble bed are shown in Figure 9. For the calculation of the experiment the steady state prior to the test was determined as described above. For the power evolution during the experiment the data from the experimental report was adopted. Other authors have already tried to recalculate the experiment with the 2D-Code THERMIX and could approximate the experimental results by

prescribing an artificial mass flow during the experiment as a boundary condition to simulate the effect of circulation between core and steam generator [20]. In the present calculation it was attempted to simulate the effect of recirculation directly. The steam generator, which represents a major heat sink, was represented inside the computational domain as a structure with constant temperature.

The initial calculated and measured temperatures and their development during the time of the experiment are shown in Figure 10. For the position of the measured points, see Figure 6. The agreement between measured and calculated temperatures is good, solely the point "Bottom Reflector" differs around 40 °C. The propagations of the other temperatures in the solid structures show qualitatively the same propagation as in the experiment, but the absolute temperatures differ up to 50° C. This may be due to a part of inaccurate the heat transfer parameters which were taken by experience.

The cooling effect due to the gas circulating between core and steam generator is qualitatively and partly also quantitatively reproduced. The solid temperatures and the flow at the end of the transient are shown in Figure 11. The convective roll in the top reflector can be clearly seen between the steam generator and the hot core.

In general, the flow to be considered here is not trivial to calculate. Heating at lower and cooling at higher elevations yields an unstable configuration with heavier above lighter gas, which gives rise to unsteady, turbulent motion. The porous medium approach with assumption of friction dominated flow as applied in ATTICA3D comes to its limits for this type of flow. The magnitude of the circulation seems to be underestimated, which can be seen from the temperature development at the graphite nose in Figure 10, especially at the top, which still shows a large difference. A possible explanation could be flow separation in azimutal direction, with helium flowing upwards in one slot and moving downwards at another slot inside the top reflector, which could result in a higher temperature drop at the graphite nose.

#### 4. Conclusion

The thermal-hydraulic code ATTICA3D is being developed as a tool for safety analyses and support of design for high temperature gas cooled reactors. A brief description of its features was given. Emphasis of the present paper was on presenting results on the validation status of the code.

Calculations with ATTICA3D were performed for a series of SANA experiments. These experiments aim at the understanding of the passive heat removal from pebble beds. Although the experiments were performed at low (i.e. atmospheric) pressure, the calculations demonstrate that the effect of natural convection flow must be considered in order to explain features of the measured temperature distributions. In general, the simulations are in good agreement with the measurements and correctly reproduce the influence of the flow on axial and radial temperature distributions for different gas atmospheres (Helium or Nitrogen). Further improvements regarding the agreement with experimental data are expected by taking into account experimental more detailed boundary conditions.

As a further example for the validation of the ATTICA3D code, results of calculations for a DLOFCA experiment in the AVR experimental reactor were presented. Since the design of the AVR reactor has genuinely tree-dimensional features, the calculations were also done in 3D. A consistent initial state for the experimental transient was obtained from coupled calculations of neutronics (using the CITATION code) and thermal-hydraulics (using ATTICA3D). The effect of natural circulation flow induced by the steam generator (still operating during the transient and acting as a major heat sink) was directly simulated. Comparison with temperatures measured during the DLOFCA transient mostly showed good agreement.

Continuation of the validation calculations is foreseen, taking into account model improvements in ATTICA3D as well as more detailed representations of experimental conditions. The heat transfer by radiation in the void above the core is going to be modelled in the future. Further improvements will be

done for the pressure drop models. More detailed material data for the heat transfer of the experiments may lead to better agreement between experiment and calculation.

Additional experiments from the SANA facility will be included, but also data from other facilities and reactors, e.g. the HTR-10.

# 5. Acknowledgement

This work was supported by the EnBW Kernkraft GmbH, additional support was provided by German Federal Ministry of Economics and Technology.

#### 6. References

- [1] U.S. DOE, 2002, "A Technology Roadmap for Generation IV Nuclear Energy Systems", Nuclear Energy Research Advisory Committee and the Generation IV International Forum.
- [2] IAEA-TECDOC-1163, "Heat Transport and Afterheat Removal for Gas Cooled Reactors under Accident Conditions", IAEA, Vienna, 2000.
- [3] S. Becker, E. Laurien, "Three-dimensional numerical simulation of flow and heat transport in high-temperature nuclear reactors", Nuclear Engineering and Design 222, pp.189-201, 2003.
- [4] K. Hossain, M. Buck, N. Ben Said, W. Bernnat, G. Lohnert, "Development of a fast 3D thermal-hydraulic tool for design and safety studies for HTRs", Nuclear Engineering and Design 238, pp. 2976–2984, 2008.
- [5] K. Hossain, M. Buck, W. Bernnat, G. Lohnert, "TH3D, A Three-dimensional thermal hydraulic Tool for design and safety analysis of HTRs", Proceedings of HTR 2008, September 28 October 1, 2008, Washington, D.C., USA.
- [6] S. Ergun, A. A. Orning, "Fluid Flow through Randomly Packed Columns and Fluidized Beds", Industrial and Engineering Chemistry, 41 (6), 1949.
- [7] The Nuclear Safety Standards Commission (Kerntechnischer Ausschuss KTA), "Reactor Core Design for High-Temperature Gas-Cooled Reactor", KTA 3102, 1983.
- [8] M. Lange, "Experimente zur selbstätigen Abfuhr der Nachwärme bei Hochtemperaturreaktoren (Experiments related to Selfoperating Removal of Decay-heat at High Temperature Reactors)", Forschungszentrum Jülich GmbH, Institut für Sicherheitsforschung und Reaktortechnik, Jül-3102, Jan. 1995.
- [9] R. Bauer, "Effektive radiale Wärmeleitfähigkeit gasdurchströmter Schüttungen mit Partikeln unterschiedlicher Form und Größenverteilung (Effective radial heat conduction of pebble beds with gas flow, particles of different sizes and forms)", VDI-Forschungshefte, 582, 1977.
- [10] A. Seubert, A. Sureda, J. Bader, J. Lapins, M. Buck, E. Laurien, "The 3-D Time-Dependent Transport Code TORT-TD and its coupling with the 3-D Thermal-Hydraulic Code ATTICA3D for HTGR-Applications", Proceedings of HTR 2010, October 18-20, 2010.
- [11] B. Stöcker, H.-F. Nießen, "Data Sets of the SANA Experiment 1994 1996", Forschungszentrum Jülich GmbH, Institut für Sicherheitsforschung und Reaktortechnik, Jül-3409, July 1997.

- [12] B. Stöcker, "Untersuchungen zur selbsttätigen Nachwärmeabfuhr bei Hochtemperaturreaktoren unter besonderer Berücksichtigung der Naturkonvektion (Investigations for Self-acting Decay Heat Transport in High Temperature Reactors under special consideration of Natural Convection)", Forschungszentrum Jülich GmbH, Institut für Sicherheitsforschung und Reaktortechnik, Jül-3504, Februar 1998.
- [13] Association of German Engineers (VDI) Society for Energy Technologies (Publ.), "AVR-Experimental High-Temperature reactor; 21 years of successful operation for a future energy technology", VDI-Verlag GmbH, Düsseldorf 1990.
- [14] E. Ziermann, G. Ivens, "Abschlußbericht über den Leistungsbetrieb des AVR Versuchskernkraftwerkes (Final Report about Operation of the AVR Experimental Nuclear Power Station)", Forschungszentrum Jülich GmbH, Arbeitsgemeinschaft Versuchsreaktor (AVR) GmbH, Jül-3448, Jülich, October 1997.
- [15] K. Verfondern, H. Nabilek, J.M. Kendall, Coated Particle Fuel for High Temperature Gas Cooled Reactors", Nuclear Engineering and Technology, Vol. 39 No.5, October 2007.
- [16] K. Krüger, "Experimentelle Simulation eines Kühlmittelverlust-Störfalls mit dem AVR-Reaktor (Experimental Simulation of a Loss-of-Coolant Accident with the AVR Reactor)", Kernforschungsanlage Jülich GmbH, Jül-2297, August 1989.
- [17] ReActor for Process heat, Hydrogen and Electricity generation (RAPHAEL). Integrated Project of the 6th Framework Programme, 2002.
- [18] T. B. Fowler, "RSICC Computer Code Collection CITATION-LDI 2", Oak Ridge National Laboratory, ORNL-TM-2496, October 1971, March 1996.
- [19] D. Mathews, "An Improved Version of the Microx-2 Code", Paul Scherer Institut, PSI Bericht Nr. 97-11, November 1997.
- [20] M. Ding, B. Boer, J.L. Kloostermann, D. Lathouwers, "Evaluation of experiments in the AVR with the DALTON-THERMIX coupled code system", Nuclear Engineering and Design 239, pp.3105–3115, 2009.